



Published in final edited form as:

Gastroenterology. 2020 September ; 159(3): 999–1014.e9. doi:10.1053/j.gastro.2020.05.056.

Agonist of RORA Attenuates Nonalcoholic Fatty Liver Progression in Mice via Up-regulation of MicroRNA 122

Chofit Chai^{1,*}, Bryan Cox^{2,*}, Dayana Yaish¹, Devora Gross¹, Nofar Rosenberg¹, Franck Amblard², Zohar Shemuelian¹, Maytal Gefen¹, Amit Korach³, Oren Tirosh⁴, Tali Lanton¹, Henrike Link¹, Joseph Tam⁵, Anna Permyakova⁵, Gunes Ozhan⁶, Jonathan Citrin¹, Haixing Liao⁷, Mirna Tannous¹, Michal Hahn⁴, Jonathan Axelrod¹, Enara Arretxe⁸, Cristina Alonso⁸, Ibon Martinez-Arranz⁸, Pablo Ortiz Betés⁸, Rifaat Safadi⁹, Ahmad Salhab⁹, Johnny Amer⁹, Zahira Tber², Seema Mengshetti², Hilla Giladi¹, Raymond F. Schinazi², Eithan Galun¹

¹Goldyne Savad Institute of Gene Therapy, Hadassah Hebrew University Hospital, Jerusalem, Israel

²Laboratory of Biochemical Pharmacology Emory University, Department of Pediatrics, Atlanta, Georgia

³Cardiothoracic Surgery, Hadassah Hebrew University Hospital, Jerusalem, Israel

⁴Institute of Biochemistry, Food Science and Nutrition, The Robert H. Smith Faculty of Agriculture, Food, and Environment, The Hebrew University of Jerusalem, Rehovot, Israel

⁵Obesity and Metabolism Laboratory, Multidisciplinary Center for Cannabinoid Research, Faculty of Medicine, The Institute for Drug Research, The Hebrew University of Jerusalem, Israel

⁶Izmir Biomedicine and Genome Center, Dokuz Eylul University Health Campus, Izmir, Turkey

⁷The First Affiliated Hospital of Guangzhou Medical University, Guangzhou, China

Correspondence Address correspondence to: Raymond F. Schinazi, Director, Laboratory of Biochemical Pharmacology & Director, HIV-Cure Scientific Working Group, Emory University Center for AIDS Research, Emory University, Atlanta, Georgia 30322. raymond.schinazi@emory.edu; or Eithan Galun, MD, Director, Goldyne Savad Institute of Gene Therapy, Hadassah Hebrew University Hospital, Jerusalem, 91120, Israel. eithang@hadassah.org.il.

* Authors share co-first authorship.

CRedit Authorship Contributions

Chofit Chai, PhD (Investigation: Lead); Bryan Cox, PhD (Investigation: Supporting); Dayana Yaish, PhD student (Investigation: Supporting); Devora Gross, MSc student (Investigation: Supporting); Nofar Rosenberg, PhD student (Investigation: Supporting); Franck Amblard, PhD (Investigation: Supporting); Zohar Shemuelian, MSc student (Investigation: Supporting); Maytal Gefen, PhD student (Investigation: Supporting); Amit Korach, MD (Investigation: Supporting); Oren Tirosh, PhD (Investigation: Supporting); Tali Lanton, PhD (Investigation: Supporting); Henrike Link, MD student (Investigation: Supporting); Joseph Tam, Prof (Investigation: Supporting); Anna Permyakova, PhD (Investigation: Supporting); Gunes Ozhan, MD (Investigation: Supporting); Jonathan Citrin, medical student (Investigation: Supporting); Haixing Liao, MD (Investigation: Supporting); Mirna Tannous, MSc student (Investigation: Supporting); Michal Hahn, PhD (Investigation: Supporting); Jonathan Axelrod, PhD (Investigation: Supporting); Enara Arretxe, PhD (Investigation: Supporting); Cristina Alonso, PhD (Investigation: Supporting); Ibon Martinez-Arranz, PhD (Investigation: Supporting); Pablo Ortiz Betés, PhD (Investigation: Supporting); Rifaat Safadi, MD (Investigation: Supporting); Ahmad Salhab, PhD student (Investigation: Supporting); Johnny Amer, PhD (Investigation: Supporting); Zahira Tber, PhD (Investigation: Supporting); Seema Mengshetti, PhD (Investigation: Supporting); Hilla Giladi, PhD (Investigation: Equal; Writing – review & editing: Equal); Raymond F. Schinazi, Prof (Conceptualization: Equal; Investigation: Equal; Writing – original draft: Equal); Eithan Galun, Prof (Conceptualization: Lead; Formal analysis: Equal; Funding acquisition: Lead; Project administration: Equal; Writing – review & editing: Equal).

Conflicts of interest

The authors disclose no conflicts.

Supplementary Material

Note: To access the supplementary material accompanying this article, visit the online version of *Gastroenterology* at www.gastrojournal.org, and at <https://doi.org/10.1053/j.gastro.2020.05.056>.

⁸OWL Metabolomics, Bizkaia Technology Park, Derio, Spain

⁹Liver Unit, Gastroenterology Institute, Department of Medicine, Hadassah Hebrew University Hospital, Jerusalem, Israel

Abstract

BACKGROUND & AIMS: Development of nonalcoholic steatohepatitis (NASH) is associated with reductions in hepatic microRNA122 (MIR122); the RAR related orphan receptor A (RORA) promotes expression of MIR122. Increasing expression of RORA in livers of mice increases expression of MIR122 and reduces lipotoxicity. We investigated the effects of a RORA agonist in mouse models of NASH.

METHODS: We screened a chemical library to identify agonists of RORA and tested their effects on a human hepatocellular carcinoma cell line (Huh7). C57BL/6 mice were fed a chow or high-fat diet (HFD) for 4 weeks to induce fatty liver. Mice were given hydrodynamic tail vein injections of a MIR122 antagonist (antagomiR-122) or a control antagomiR once each week for 3 weeks while still on the HFD or chow diet, or intraperitoneal injections of the RORA agonist RS-2982 or vehicle, twice each week for 3 weeks. Livers, gonad white adipose, and skeletal muscle were collected and analyzed by reverse-transcription polymerase chain reaction, histology, and immunohistochemistry. A separate group of mice were fed an atherogenic diet, with or without injections of RS-2982 for 3 weeks; livers were analyzed by immunohistochemistry, and plasma was analyzed for levels of aminotransferases. We analyzed data from liver tissues from patients with NASH included in the RNA-sequencing databases GSE33814 and GSE89632.

RESULTS: Injection of mice with antagomiR-122 significantly reduced levels of MIR122 in plasma, liver, and white adipose tissue; in mice on an HFD, antagomiR-122 injections increased fat droplets and total triglyceride content in liver and reduced β -oxidation and energy expenditure, resulting in significantly more weight gain than in mice given the control microRNA. We identified RS-2982 as an agonist of RORA and found it to increase expression of MIR122 promoter activity in Huh7 cells. In mice fed an HFD or atherogenic diet, injections of RS-2982 increased hepatic levels of MIR122 precursors and reduced hepatic synthesis of triglycerides by reducing expression of biosynthesis enzymes. In these mice, RS-2982 significantly reduced hepatic lipotoxicity, reduced liver fibrosis, increased insulin resistance, and reduced body weight compared with mice injected with vehicle. Patients who underwent cardiovascular surgery had increased levels of plasma MIR122 compared to its levels before surgery; increased expression of plasma MIR122 was associated with increased levels of plasma free fatty acids and levels of RORA.

CONCLUSIONS: We identified the compound RS-2982 as an agonist of RORA that increases expression of MIR122 in cell lines and livers of mice. Mice fed an HFD or atherogenic diet given injections of RS-2982 had reduced hepatic lipotoxicity, liver fibrosis, and body weight compared with mice given the vehicle. Agonists of RORA might be developed for treatment of NASH.

Keywords

NAFLD; Lipid; Metabolism; Obesity

Nonalcoholic fatty liver disease (NAFLD) is the most common chronic disease worldwide, affecting more than 25% of the global population.¹ NAFLD is associated with increased cardiovascular diseases and diabetes, with 30% of patients progressing to chronic liver inflammation termed *nonalcoholic steatohepatitis (NASH)*, followed by fibrosis and cirrhosis within 10–30 years. NASH can also progress to hepatocellular carcinoma (HCC) in 15% of the cases, and it is the second-leading cause of cancer-related death worldwide.² NASH is tightly associated with metabolic syndrome, which includes obesity, diabetes, hypertension, hypertriglyceridemia, and reduced high-density lipoprotein cholesterol levels. Although NASH is a major health care burden, there is currently no approved therapy reversing NASH and its consequences.³ A number of compounds were recently developed for NAFLD/NASH treatment, some in phase 2 and phase 3 trials. However, to date, none of these compounds has shown a therapeutic effect in all of the clinical aspects of NASH, including lipotoxicity, inflammation, fibrosis, insulin resistance, and obesity.

The liver-specific microRNA-122 (MIR122) is associated with hepatic lipid metabolism.⁴ Its level decreases in livers of humans with NASH⁵ and increases in the blood of these patients. In accordance with this, it was shown that MIR122-knockout mice develop NASH that later progresses to HCC.^{6,7} We have shown that MIR122 is induced by free fatty acids (FFAs), and this induction is mediated by the activation of hepatic RORA. The increase in hepatic MIR122 by the FFA-RORA machinery leads to suppression of triglycerides (TG) because of targeting and reducing the levels of enzymes involved in TG biosynthesis by MIR122.⁸

Based on these results, we have undertaken an approach to determine whether activating RORA could reverse phenotypes associated with NAFLD. Toward this aim, we engineered a panel of new RORA agonists and selected 1 compound based on its significant effect of activating the MIR122 promoter. This activation caused beneficial effects on lipotoxicity in the livers of mouse models, including reduced liver inflammation and reversed fibrosis. Furthermore, this RORA agonist reduced remote adipose tissue inflammation, improved insulin resistance, and reduced the body weight of the obese mice.

Materials and Methods

Cell Culture

The human hepatocellular carcinoma cell line Huh7 was cultured in Dulbecco's modified Eagle medium supplemented with 10% fetal calf serum, 1% penicillin/streptomycin (Thermo Fisher Scientific, Waltham, MA). Cells were cultured at 37°C in a humidified atmosphere containing 5% CO₂, except for an experiment in which cells were placed in 32°C, as indicated in the text.

Plasmids

The human MIR122 promoter fragments spanning the region from –900 base pairs relative to the transcription start site and mutating the RORA binding site (plasmids pMIR122-900 and pMIR122-RORA mut, respectively) were generated as described previously.⁸

Transfections

For luciferase assays, cells grown in 24-well plates were cotransfected with a luciferase reporter plasmid (50 ng) and 1 ng of *Renilla* luciferase vector (PRL, Promega, Madison, WI) with Lipofectamine LTX (Invitrogen, Waltham, MA) transfection reagent. For all experiments, the transfection performed using serum-free medium (Opti-MEM; catalog no. 31985070; Thermo Fisher Scientific).

Luciferase Activity Assay

After transfections, the cells were lysed with passive lysis buffer (catalog no. E1941, Promega), shaken for 20 minutes at room temperature, and transferred into the appropriate 96-well plate. Firefly and *Renilla* luciferase activity was assessed using the Dual Luciferase Reporter Assay system (catalog no. E1910, Promega) on a luminometer Mithras 2000 (Centro XZ, LB960; Berthold Technologies, Bad Wildbad, Germany). The luciferase activity was normalized to *Renilla* luciferase activity. Readings were taken in triplicate.

RORA Agonist Treatments

Commercial RORA agonist SR1078 (Cayman Chemical, Ann Arbor, MI) and our newly synthesized RORA compound stocks were prepared by dissolving in dimethyl sulfoxide (DMSO) (1 mg/mL). Huh7 cells were treated overnight with 10 $\mu\text{mol/L}$ SR1078 or with 1 $\mu\text{mol/L}$ of all other tested compounds. DMSO alone (0.2%) was used as control. The RORA agonist RS-2982 was dissolved in saline and up to 5% DMSO and was injected intraperitoneally to mice in the dosage according to the text.

RNA Extraction and Quantitative Real-Time Reverse-Transcription Polymerase Chain Reaction

Total RNA, including small RNAs, was isolated from 200 μL of plasma or culture media samples using the miRNeasy Mini kit (Qiagen, Valencia, CA) with 2 minor modifications. First, 200 μL of plasma or culture media was lysed with 1 mL of Qiazol solution (Qiagen, Valencia, CA). Second, 50 pmol/L of synthesized single-strand *Caenorhabditis elegans* microRNA (miRNA) (*C. elegans* miR-39) was added as the spike-in control to monitor extraction efficiency. The remainder of the RNA extraction was performed according to the manufacturer's instructions. miRNAs were eluted with 30 μL of RNase-free water. Total RNA, including miRNAs, from cells or tissues were isolated using TRIzol reagent (Invitrogen). Complementary DNA (cDNA) was synthesized by using the Quanta BioSciences (Beverly, MA) qScript cDNA Synthesis Kit (95047-100) for messenger RNA (mRNA) analysis and the qScript microRNA cDNA Synthesis Kit (95107-100) for miRNA analysis. Quantitative real-time reverse-transcription polymerase chain reaction (qRT-PCR) of miRNAs and mRNA was performed with the ABI 7900 HT Real-Time PCR System and a SYBR Green PCR Kit (Quanta catalog nos. 84018 and 84071, respectively). The fold expression and statistical significance were calculated using the $2^{-\text{Ct}}$ method. All samples from 1 experiment were performed in triplicate. The primers used for qRT-PCR are shown in Supplementary Table 1.

Animal Studies

Male C57BL/6 mice, 7–8 weeks old, were purchased from Harlan Laboratories (Jerusalem, Israel). All mice were kept in a pathogen-free facility under a 12-hour light/dark cycle. Mice were handled according to the criteria outlined in the “Guide for the Care and Use of Laboratory Animals” prepared by the National Academy of Sciences and published by the National Institutes of Health. Research on mice was approved by the Hebrew University Institutional Animal Care and Ethics Committee (ethics number MD-15-14423-3).

AntagoMIR122 Treatment of High Fat Diet–Fed Mice

C57BL/6 mice, 7–8 weeks old, were fed chow or 50% high-fat diet (HFD) consisting of 50% fat, 20% sucrose, 10% fructose, and 1.25% cholesterol (Envigo, TD.150235, Indianapolis, IN) for 4 weeks. In experiments of MIR122 repression by antagoMIR, mice were hydrodynamic tail vein injected with antagoMIR122 or antagoMIR-control (5 μ g/mouse in 1.5 mL saline) once a week for 3 weeks and were still fed HFD or chow diet. After 3 weeks of injections, mice were killed, and the livers, gonadal white adipose, and skeletal muscle tissues were frozen in liquid nitrogen or in optimum cutting temperature–embedded frozen blocks for further RNA and histologic analysis. AntagoMIRs were obtained from Sigma-Aldrich (St Louis, MO) (see Supplementary Table 2).

Statistical Analysis

Data were subjected to statistical analysis using the Excel software package (Microsoft, Redmond, WA) or GraphPad Prism6 (GraphPad Software Inc, La Jolla, CA). Two-tailed Student *t* tests and Pearson and Spearman correlation coefficients were used to determine the difference between the groups. Data are given as mean \pm standard deviation (SD) and are shown as error bars for all experiments. Differences were considered significant at $P < .05$. The reported data were obtained from at least 3 biological replicates.

Additional methods, including RS-2982 and antagoMIR122 treatment of HFD- or atherogenic diet-fed mice, multiparameter metabolic assessment, Oil Red O staining, immunofluorescent staining for natural killer (NK) cells, triglycerides, FFA and β -hydroxybutyrate quantification, human blood samples and heparin elimination, RNA sequencing and bioinformatics analysis, insulin tolerance test, tissue histology and immunohistochemistry, general chemical procedures, and immunofluorescent staining for NK cells, are available in the Supplementary Materials section.

Results

The Effect of MicroRNA 122 on Lipid Metabolism in Mice Fed With a High-Fat Diet

Initially, we were interested in studying the function of MIR122 in livers of mice under HFD that cause lipotoxicity. It was previously shown in humans that MIR122 levels in livers with NASH are significantly lower.⁵ In our previous report, we showed that MIR122 reduces TG accumulation by targeting the AGPAT1 and DGAT1 enzymes in the TG biosynthesis pathway.⁸ To test the effect of reducing MIR122 in livers of HFD-fed mice, we administered to the liver by a hydrodynamic tail-vein injection antagoMIR122, which blocks and degrades MIR122 in hepatocytes⁹ (Figure 1A). This injection caused the reduction of mature MIR122

levels in the livers of mice fed with normal diet (ND) and also in HFD-fed mice (Figure 1B). The levels of MIR122 precursors, pri- and pre-MIR122, were also reduced (Figure 1C). Furthermore, antagoMIR122 injection significantly reduced the plasma level of MIR122 compared to miR-93, which was not affected (Figure 1D). Antago-MIR122 injection also reduced MIR122 levels in the remote white adipose tissue (WAT) (Figure 1E). As opposed to MIR122, the level of miR-126 in WAT was reduced in HFD mice compared to ND, and reducing MIR122 levels by antagoMIR122 caused a small, nonsignificant increase in miR-126 levels. We previously showed that reduction of mature MIR122 levels in WAT and in muscle is a result of reduced secretion of MIR122 from hepatocytes and not due to reduced MIR122 expression in nonliver tissues.⁸ The reduction of plasma MIR122 levels after antagoMIR122 injection was associated with an increase of liver fat droplets (Figure 1F) and total TG liver content (Figure 1G), as well as an increase in muscle TG levels (Figure 1H). The biochemical effect of liver MIR122 reduction was manifested by a decrease in β -oxidation (reduced plasma levels of β -hydroxybutyrate) (Figure 1I), as well as decreased liver Cpt1 α levels (carnitine palmitoyltransferase 1A), an important enzyme in the β -oxidation pathway (Figure 1J), and a reduced plasma level of FFAs (Figure 1K). All of these are known indications of an increase in TG storage in tissues and reduced energy expenditure. Blocking of MIR122 by antagoMIR122 had an overall effect on mouse weight, which increased significantly in HFD mice (Figure 1L). Liver weight also increased (Figure 1M), as was the liver-to-body weight index (Figure 1N). The effects of reducing MIR122 in the liver and systemically in remote tissues led to an increase in liver lipids and a decrease in β -oxidation and energy expenditure and had a systemic influence, altogether simulating features of the metabolic syndrome.

Reduced RORA Messenger RNA Levels in Patients With Nonalcoholic Steatohepatitis and Their Effect on RORA and MIR122 Target Genes

In our previous report, we showed that in mice, RORA regulates MIR122 expression and that this is mediated through FFAs.⁸ To study the potential relevance to human metabolism and NASH, we initially investigated human NASH data sets^{10,11} (GSE33814 and GSE89632, respectively). As shown in Figure 2A, RORA is reduced in patients with NASH. Furthermore, RORA target genes (Arg1 and CD36) are decreased in these samples (Figure 2B), and their expression is positively correlated with RORA (Figure 2C). On the other hand, the expression levels of genes that are involved in FFA biosynthesis pathways and are associated with fatty liver (Fasn and Srebf1)^{12,13} and are negatively correlated with RORA (Figure 2D). Similarly, MIR122 target genes (AldoA, ADAM17, and Agpat1) are also negatively correlated with RORA expression (Figure 2E), and their levels increase in human livers upon decreased RORA levels (Figure 2F). The expression of Fgf21 (fibroblast growth factor 21), a known target of RORA,¹⁴ is positively correlated with pre-MIR122 levels, suggesting coregulation (Figure 2G). RNA-sequencing databases (GSE101934 and GSE124731) indicate that RORA levels in hepatocytes and immune cells are comparable (Figure 2H).

Recently, it was shown that liver Fgf21 is up-regulated upon cold exposure.¹⁵ We reasoned that this could be due to increased RORA levels in the cold. To assess this assumption, we transfected Huh7 human HCC cells with a RORA reporter plasmid expressing luciferase

from the MIR122 promoter that harbors a RORA binding site. As shown in Supplementary Figure 1A-C, MIR122 expression increased when the temperature was reduced to 32°C. When the RORA consensus binding sequence in the MIR122 promoter was mutated,⁸ the increase in MIR122 expression was abolished. In addition, levels of MIR122 and its activity on target genes increased in response to cold exposure of Huh7 cells.

To investigate further the RORA-MIR122 circuitry in humans, we conducted a human study (Hadassah University Hospital institutional review board approval no. HMO-0025-18) in which we measured MIR122 plasma levels in humans undergoing major blood vessel cardiovascular surgery with the use of a cardiopulmonary machine and systemic body cooling (Supplementary Table 3). We found a significant increase in plasma MIR122 levels upon temperature reduction that positively correlated with increased plasma FFA levels. In addition, lipidomic analysis showed that plasma samples taken after body cooling contained decreased levels of a high number of TG species (Supplementary Figure 1D-G) and Supplementary Table 4).

The Effect of a Newly Identified RORA Agonist RS-2982 on Liver and Systemic MIR122 Levels in Mice

The results reported here verify our previously identified FFA-MIR122-TG metabolic circuit.⁸ Thus, we reasoned that if we increase RORA activity, it will lead to increased hepatic MIR122 expression, which will have beneficial effects on NASH as well as a systemic therapeutic effects, such as improving insulin resistance and reducing adipose tissue and body mass. To this end, we sought to identify novel RORA agonists.

A targeted virtual screen was used to identify novel RORA agonists. A set of 300,000 drug-like commercially available compounds were docked and scored into the crystal structure of the RORA ligand-binding domain complexed with cholesterol sulfate. A final set of 10 compounds was selected for activity testing. This set of compounds was assayed for their induction of the MIR122 promoter using a luciferase promoter reporter plasmid (Figure 3A). Notably, compound 1 (named RS-2982) was the most potent at inducing MIR122 promoter (Figure 3B and C), more potent than the commercial synthetic RORA agonist SR1078. Next, the toxicity profile of RS-2982 was determined by using a panel of cell lines. Compared to cycloheximide (+ control), RS-2982 had only moderate toxicity in CEM and Huh-7 ($CC_{50} = 11.0$ and $10.4 \mu\text{mol/L}$, respectively) (Supplementary Table 5). The chemical identity of this agent was confirmed by resynthesis. RS-2982 was further tested in a follow-up assay in which the RORA DNA response element in the MIR122 promoter was mutated. Consistent with RORA-specific activity, RS-2982 exhibited no induction of the mutated MIR122 promoter as opposed to the wild-type promoter (Figure 3D). When Huh7 cells were exposed to RS-2982 for 16 hours, cellular MIR122 levels did not change, but a significant amount of MIR122 was secreted to the medium (Figure 3E). In addition, there was no apparent toxicity to the cells as measured by lactate dehydrogenase (LDH) release (data not shown). Importantly, we also show that RS-2982 treatment increases MIR122 promoter activity in mice and that it is mediated by RORA, because a MIR122 reporter plasmid carrying a mutation in the RORA binding site exhibited reduced promoter activity compared to the wild-type promoter (Supplementary Figure 2).

To show further that RS-2982 is a potent inducer in mice, MIR122 levels were monitored over time in mice after a single administration of the compound (Figure 3F). MIR122 levels increased in the liver and plasma (Figure 3G and H) and was associated with an increase in the levels of hepatic MIR122 precursor's (pri-MIR122 and pre-MIR122), as well as a decrease of a known target of MIR122, AldoA, and an increase in G6Pase, a known RORA target gene¹⁶ (Figure 3I). As seen in Figures 3J-L, after single administration of RS-2982, mature MIR122 levels increased significantly in WAT, muscle, and heart tissues. Furthermore, in the heart tissue, 3 MIR122 target genes were significantly down-regulated (Figure 3M). These data show that RS-2982 is a potent inducer of MIR122 in mice.

RS-2982 Reduces Body Weight and Steatosis Via Increased MicroRNA 122 Expression in High-Fat Diet–Fed Mice

As was shown in Figure 2, steatohepatitis in humans is correlated with reduced RORA levels. In accordance, mice fed with an HFD had a temporal stepwise reduction in hepatic RORA levels. Interestingly, addition of the RS-2982 agonist increased the RORA level to its level in mice fed an ND (Figure 4A). We investigated further the mechanism of action of MIR122 and RS-2982 on NAFLD to learn whether they are aligned at the same pathway. We therefore designed an experiment in which RS-2982 was injected together with the MIR122 inhibitor, antagoMIR122, to mice with NAFLD. Mice were fed with a 50% HFD, and after 4 weeks, when fatty liver was already established, they were treated with RS-2982, antagoMIR122, or both compounds together for an additional 3 weeks (Figure 4B). AntagoMIR122 was given once a week, because of a prolonged half-life time, and RS-2982 was given twice weekly, because of a plasma $t_{1/2}$ of 2.7 hours. The weighing of mice began at week 3, 1 week before treatments were initiated (Figure 4C). Control mice (antagoMIR control once a week and DMSO diluted in saline twice a week) had a steady increase in body weight; however, mice administered antagoMIR122 had the highest increase in weight. In contrast, mice treated with the RORA agonist RS-2982 exhibited a significant decrease in body weight. The weight of mice administered both antagoMIR122 and RS-2982 returned exactly to that of control animals (Figure 4C). None of the mice exhibited signs of toxicity, manifested by behavioral change. Upon cessation of the experiment, in antagoMIR122-treated animals, body weight exhibited a significant increase, indicating that reduction of MIR122 in the liver is associated with a systemic effect, whereas the administration of RS-2982 significantly reduced mouse weight (Figure 4D). The liver weight of the mice was in accordance with their body weight (Figure 4E). The liver was further analyzed to assess lipotoxicity and, as shown in Figure 4F, hepatic lipid droplets and TG content were reduced in RS-2982-treated mice, and this reduction was completely abolished in antagoMIR122-injected mice, suggesting that the beneficial effect of RS-2982 on steatosis is mediated by MIR122 activity. We also measured a surrogate marker for energy expenditure, β -hydroxybutyrate, and found a decrease in energy expenditure upon reduction of MIR122 levels and an increase upon treatment with RS-2982 (Figure 4G). These effects were associated with reduced mature MIR122 levels in the liver, plasma, and muscle tissues upon administration of antagoMIR122 and an increase of MIR122 when RS-2982 was administered, as seen in plasma and muscle (Figure 4H-J). In agreement with our previous results, pri-MIR122 was not detected in muscle tissue (Supplementary Table 6), indicating that mature MIR122 is not expressed from the endogenous MIR122 promoter. The effect on

muscle MIR122 levels was very similar to that seen in the plasma and was probably through MIR122 secretion effects. The level of mature MIR122 in the liver showed no increase after RS-2982 administration (Figure 4H), probably due to its secretion to the plasma because the MIR122 precursor RNAs, pri- and pre-MIR122, increased significantly in the liver after RS-2982 administration (Figure 4K). The MIR122 target gene *Dgat1* was reduced in the liver after RS-2982 treatment, whereas the RORA target gene *Fgf21* increased (Figure 4L). The MIR122 target genes in the muscle, *AldoA* and *Agpat1*, were also affected in a respective manner (Figure 4M). Furthermore, in the presence of RS-2982, the muscle TG levels were reduced (Figure 4N). The level of the liver *Fgf21* mRNA correlated with pri-MIR122 levels after RS-2982 administration, suggesting a coregulation (Figure 4O). These observations support our hypothesis that controlling MIR122 levels, either by reducing its hepatic levels by antagoMIR122 or increasing it by RS-2982 has both liver/ central and remote/peripheral effects. Thus, the overall effects of RS-2982 culminate in a significant weight reduction associated with reduced lipotoxicity.

The RORA Agonist RS-2982 Reduces Steatosis Via Increased MicroRNA 122 Expression in High-Fat Diet–Fed Mice

After we have shown that RS-2982 is a potent MIR122 activator that exhibits beneficial biochemical effects, we aimed to determine its effect on lipotoxicity and metabolism. RS-2982 was administered to mice with an established NAFLD (following HFD feeding) (Figure 5A), which resulted in increased liver and plasma mature MIR122 levels and in increased MIR122 precursors and RORA targets in the liver (Figure 5B and C), similar to its effect on ND-fed mice (Figure 3I).

Furthermore, in this NAFLD model, RS-2982 significantly reduced the body weight of mice fed an HFD (Figure 5D and E). This effect is also apparent in the reduced percentage of liver weight from total body weight (Figure 5F). Importantly, the RORA activator significantly reversed the lipotoxic effect of mouse livers and their TG content (Figure 5G). RS-2982, which induces MIR122 production and secretion from hepatocytes, also had an effect on reducing WAT inflammation (Figure 5H). These beneficial histologic and biochemical effects were also associated with an improvement in insulin tolerance (Figure 5I). To further assess the metabolic effects of RS-2982, mice were kept in metabolic cages. Because of the potential diurnal variation of RORA,¹⁷ we focused on the relevant time of day (9:00 AM and 11:00 AM). As is apparent from Figure 5J, total energy expenditure as well as fat oxidation, increased in the RS-2982–treated mice.

The Anti-inflammatory and Anti-fibrogenic Effects of Activating the RORA–MicroRNA 122–Triglyceride Circuitry With RS-2982

After our findings that the RORA activator RS-2982 displays significant metabolic benefits, we wanted to investigate its effects on liver inflammation and fibrosis. Toward this aim, we used the mouse atherogenic diet model.¹⁸ After 3 weeks on the atherogenic diet, when liver inflammation and fibrosis had already developed, we initiated treatment with RS-2982 for additional 3.5 weeks, with 3 injections per week (Supplementary Table 7 and Figure 6A). Animals were then assessed for the effect of RS-2982 on a large number of processes. RS-2982 improved liver enzymes, significantly reducing aspartate aminotransferase and

alanine aminotransferase levels (Figure 6B). Mature MIR122 levels increased in the liver and in the plasma after the administration of RS-2982 (Figure 6C). H&E, CD3m and F4/80 staining (Figure 6D) show that RS-2982 improved liver inflammation significantly. This improvement in inflammation was associated with a significant reduction in liver fibrosis, as assessed by 2 measures, Masson trichrome and α -smooth muscle actin staining (Figure 6E). NK cells are known to target activated liver stellate cells.¹⁹ The resolution of fibrosis was associated with a significant reduction in NK cells in the livers of RS-2982-treated mice (Figure 6E). The effect of the RORA activator RS-2982 was apparent also on fibrosis driver genes, as seen in Figure 6F. These results, summarized in our model in Figure 7, strongly support the concept that RORA agonists reduce hepatic inflammation and fibrosis, likely through MIR122 up-regulation.

Discussion

In this report, we show that activating RORA has a major beneficial effect on NAFLD and on associated metabolic syndromes, both on liver pathologies and on peripheral tissues. This RORA activity is mediated through induction of hepatic MIR122 levels, although additional RORA activities could potentially contribute to these beneficial effects. MIR122, in turn, suppresses hepatic lipotoxicity by targeting the expression of central enzymes in TG biosynthesis. RORA activation also results in increased secretion of hepatic MIR122 to the plasma, leading to an increase in its level in remote tissues such as WAT, muscle, and heart muscle, where MIR122 also affects its target genes. Hence, activation of RORA has both a liver and a systemic effect.

It should be noted that RORA was associated with numerous developmental and pathologic neurologic conditions. RORA is expressed in many brain tissues, including the cerebellum, pineal gland, and hippocampus, and was shown to be associated with autism and cerebral ataxia.²⁰ RORA activation also exerts its effect on specific types of cells in the brain, including Purkinje cells and astrocytes.²¹ We have monitored in our experiments the animals that were treated with RS-2982 and could not detect any gross neurologic major abnormalities.

We identified the synthetic RORA activator RS-2982 among a number of compounds by its strong enhancement of MIR122 promoter activity. By testing the effect of RS-2982 in several mice models, we found this compound to have a significant beneficial effect on metabolism, including reducing fat in fatty liver, suppressing liver inflammation associated with hepatic lipotoxicity, reversal of liver fibrosis, improving insulin resistance, and reducing body weight of HFD mice.

Therapy for NASH has a high priority because it is widespread worldwide and because, today, there is not a single approved drug for NASH, although many drugs are prescribed for specific maladies associated with the metabolic syndrome and NASH.²² Therefore, patients with NASH are still without a therapeutic option other than proposing that they follow a specific diet, such as a Mediterraneanstyle diet, that improves NAFLD to some extent.²³ Many compounds are in the drug development pipeline, some showing interesting promise,²⁴ and some failing to meet important endpoints.²⁵ A number of previous reports and our

study point to the potential of hijacking the mechanistic action of MIR122 as an antilipotoxic effector in the liver. We decided to investigate the potential therapeutic effects of MIR122 because of its hormone-like features. Namely, MIR122, like many other microRNAs, is produced in 1 tissue, the liver, and is then secreted to the blood, from where it reaches remote tissues. We have shown that MIR122 exerts its antilipemic effect in the liver and in remote tissues.

Hepatocytes produce large amounts of MIR122, reaching 250,000 copies per cell. The effective remote activity of MIR122 correlates with its high production and secretion to generate high plasma levels. Therefore, inducing a high production rate of MIR122 could be translated into an effective therapeutic compound. However, rather than developing a system in which a synthetic MIR122 (mimic-MIR122) is synthesized, made as a drug, and injected to patients with NASH for years, we preferred to develop a small drug that induces the endogenous expression of the hepatic MIR122 and could be given to patients for a prolonged period.

It should be noted that MIR122 has additional therapeutic properties that are relevant to NASH. Both strands of the initial MIR122 duplex, MIR122-5p and MIR122-3p (MIR122*), have tumor-suppressive effects.²⁶⁻²⁸ For patients with NASH, these activities of MIR122 offer additional therapeutic benefits, which adds to the motivation to develop pro-MIR122-based compounds into drugs.²⁹

In this report, we show that the RS-2982 compound that we developed has substantial anti-NASH activity in mice. It specifically activates RORA, which, in turn, increases MIR122 levels in the liver. MIR122 is secreted from the liver and reaches other organs, including adipose tissue, and represses TG synthesis, and that results in a metabolic shift from fat accumulation to energy expenditure. Based on our results, we propose that RORA activators are promising compounds to be developed and assessed for their clinical beneficial effects on NAFLD in patients.

Supplementary Material

Refer to Web version on PubMed Central for supplementary material.

Acknowledgments

The authors wish to thank Yuval Nevo, Sharona Elgavish, and the Hadar Benyamini Bioinformatics Unit of the Israeli Centers of Research Excellence (I-CORE) Computation Center, The Hebrew University and Hadassah Hebrew University Hospital, Jerusalem, for the bioinformatic analysis conducted during the project; Devorah Olam for the histologic analysis conducted in this project; Jörg Heeren and Anna Worthmann for collaboration and discussion; and Israel Voldavsky, who gave us the protocol for the use of heparinase for eliminating heparin from the human samples.

Funding

This work was supported by an ERC advance (GA no. 786575) RxmiRcancer (to Eithan Galun), Deutsche Forschungsgemeinschaft SFB841 project C3 (to Eithan Galun), National Institutes of Health CA197081-02 (to Eithan Galun), MOST (to Eithan Galun), ISF collaboration with Canada (2473/2017) (to Eithan Galun), personal ISF (486/2017) (to Eithan Galun), ICORE-ISF (41/2011) (to Eithan Galun), DKFZ-MOST (to Eithan Galun), the Robert H. Benson Living Trust, and Selma Kron Foundation to student fellowships.

Abbreviations used in this paper:

cDNA	complementary DNA
DMSO	dimethyl sulfoxide
FFA	free fatty acid
HCC	hepatocellular carcinoma
HFD	high-fat diet
miRNA	microRNA
MIR122	microRNA 122
mRNA	messenger RNA
NAFLD	nonalcoholic fatty liver disease
NASH	nonalcoholic steatohepatitis
ND	normal diet
NK	natural killer
qRT-PCR	quantitative real-time reverse-transcription polymerase chain reaction
SD	standard deviation
TG	triglycerides
WAT	white adipose tissue

References

1. Younossi ZM, Blisset D, Blisset R, et al. The economic and clinical burden of nonalcoholic fatty liver disease in the United States and Europe. *Hepatology* 2016;64:1577–1586. [PubMed: 27543837]
2. Younossi Z, Anstee QM, Marietti M, et al. Global burden of NAFLD and NASH: trends, predictions, risk factors and prevention. *Nat Rev Gastroenterol Hepatol* 2018;15:11–20. [PubMed: 28930295]
3. Konerman MA, Jones JC, Harrison SA. Pharmacotherapy for NASH: current and emerging. *J Hepatol* 2018;68:362–375. [PubMed: 29122694]
4. Esau C, Davis S, Murray SF, et al. miR-122 regulation of lipid metabolism revealed by in vivo antisense targeting. *Cell Metab* 2006;3:87–98. [PubMed: 16459310]
5. Cheung O, Puri P, Eiken C, et al. Nonalcoholic steatohepatitis is associated with altered hepatic microRNA expression. *Hepatology* 2008;48:1810–1820. [PubMed: 19030170]
6. Tsai WC, Hsu HD, Hsu CS, et al. MicroRNA-122 plays a critical role in liver homeostasis and hepatocarcinogenesis. *J Clin Invest* 2012;122:2884–2897. [PubMed: 22820290]
7. Hsu SH, Wang B, Kota J, et al. Essential metabolic, anti-inflammatory, and anti-tumorigenic functions of miR-122 in liver. *J Clin Invest* 2012;122:2871–2883. [PubMed: 22820288]
8. Chai C, Rivkin M, Berkovits L, et al. Metabolic circuit involving free fatty acids, microRNA 122, and triglyceride synthesis in liver and muscle tissues. *Gastroenterology* 2017;153:1404–1415. [PubMed: 28802563]

9. Krützfeldt J, Rajewsky N, Braich R, et al. Silencing of microRNAs in vivo with ‘antagomirs’. *Nature* 2005; 438(7068):685–689. [PubMed: 16258535]
10. Arendt BM, Comelli EM, Ma DWL, et al. Altered hepatic gene expression in nonalcoholic fatty liver disease is associated with lower hepatic n-3 and n-6 polyunsaturated fatty acids. *Hepatology* 2015;61:1565–1578. [PubMed: 25581263]
11. Starmann J, Falth M, Spindelbock W, et al. Gene expression profiling unravels cancer-related hepatic molecular signatures in steatohepatitis but not in steatosis. *PLoS One* 2012;7(10):e46584. [PubMed: 23071592]
12. Dorn C, Riener MO, Kirovski G, et al. Expression of fatty acid synthase in nonalcoholic fatty liver disease. *Int J Clin Exp Pathol* 2010;3:505–514. [PubMed: 20606731]
13. Knebel B, Haas J, Kotzka J, et al. Liver-specific expression of transcriptionally active SREBP-1c is associated with fatty liver and increased visceral fat mass. *PLoS One* 2012;7(2):e31812. [PubMed: 22363740]
14. Wang Y, Solt LA, Burris TP. Regulation of FGF21 expression and secretion by retinoic acid receptor-related orphan receptor a. *J Biol Chem* 2010;285:15668–15673. [PubMed: 20332535]
15. Ameka M, Markan KR, Morgan DA, et al. Liver derived FGF21 maintains core body temperature during acute cold exposure. *Sci Rep* 2019;9(1):630. [PubMed: 30679672]
16. Chauvet C, Vanhoutteghem A, Duhem C, et al. Control of gene expression by the retinoic acid-related orphan receptor alpha in HepG2 human hepatoma cells. *PLoS One* 2011;6(7):e22545. [PubMed: 21818335]
17. Nguyen TT, Mattick J, Yang Q, et al. Bioinformatics analysis of transcriptional regulation of circadian genes in rat liver. *BMC Bioinformatics* 2014;15:83. [PubMed: 24666587]
18. Anavi S, Eisenberg-Bore M, Hahn-Obercyger M, et al. The role of iNOS in cholesterol-induced liver fibrosis. *Lab Invest* 2015;95:914–924. [PubMed: 26097999]
19. Krizhanovsky V, Yon M, Dickins RA, et al. Senescence of activated stellate cells limits liver fibrosis. *Cell* 2008; 134:657–667. [PubMed: 18724938]
20. Guissart C, Latypova X, Rollier P, et al. Dual molecular effects of dominant RORA mutations cause two variants of syndromic intellectual disability with either autism or cerebellar ataxia. *Am J Hum Genet* 2018;102:744–759. [PubMed: 29656859]
21. Journiac N, Jolly S, Jarvis C, et al. The nuclear receptor RORa exerts a bi-directional regulation of IL-6 in resting and reactive astrocytes. *Proc Natl Acad Sci U S A* 2009; 106:21365–21370. [PubMed: 19955433]
22. Wattacheril J, Issa D, Sanyal A. Nonalcoholic steatohepatitis (NASH) and hepatic fibrosis: emerging therapies. *Annu Rev Pharmacol Toxicol* 2018;58:649–662. [PubMed: 29058997]
23. Marchesini G, Petta S, Dalle Grave R. Diet, weight loss, and liver health in nonalcoholic fatty liver disease: pathophysiology, evidence, and practice. *Hepatology* 2016; 63:2032–2043. [PubMed: 26663351]
24. Friedman SL, Ratziu V, Harrison SA, et al. A randomized, placebo-controlled trial of cenicriviroc for treatment of nonalcoholic steatohepatitis with fibrosis. *Hepatology* 2018;67:1754–1767. [PubMed: 28833331]
25. Loomba R, Kayali Z, Nouredin M, et al. GS-0976 reduces hepatic steatosis and fibrosis markers in patients with nonalcoholic fatty liver disease. *Gastroenterology* 2018;155:1463–1473. [PubMed: 30059671]
26. Simerzin A, Zorde-Khvaleyevsky E, Rivkin M, et al. The liver-specific microRNA-122*, the complementary strand of microRNA-122, acts as a tumor suppressor by modulating the p53/mouse double minute 2 homolog circuitry. *Hepatology* 2016;64:1623–1636. [PubMed: 27302319]
27. Luna JM, Barajas JM, Teng KY, et al. Argonaute CLIP defines a deregulated miR-122-bound transcriptome that correlates with patient survival in human liver cancer. *Mol Cell* 2017;67:400–410. [PubMed: 28735896]
28. Sun H-L, Cui R, Zhou JK, et al. ERK activation globally downregulates miRNAs through phosphorylating exportin-5. *Cancer Cell* 2016;30:723–736. [PubMed: 27846390]
29. Bandiera S, Pfeffer S, Baumert TF, Zeisel MB. miR-122 – a key factor and therapeutic target in liver disease. *J Hepatol* 2015;62:448–457. [PubMed: 25308172]

WHAT YOU NEED TO KNOW

BACKGROUND AND CONTEXT

Development of non-alcoholic steatohepatitis is associated with reduced hepatic expression of microRNA122 (MIR122), which is regulated by the Retinoic acid receptor related orphan receptor A (RORA). Increasing expression of RORA in livers of mice increases expression of MIR122 and reduces lipotoxicity.

NEW FINDINGS

The authors identified the compound RS-2982 as an agonist of RORA that increases expression of MIR122 in cell lines and livers of mice. Mice on high-fat or atherogenic diets given injections of RS-2982 had reduced hepatic lipotoxicity, liver fibrosis, skeletal muscle triglyceride levels and body weight, compared with mice injected with vehicle.

LIMITATIONS

This study was performed in mice; additional studies are needed in humans.

IMPACT

Agonists of RORA might be developed for treatment of NASH.

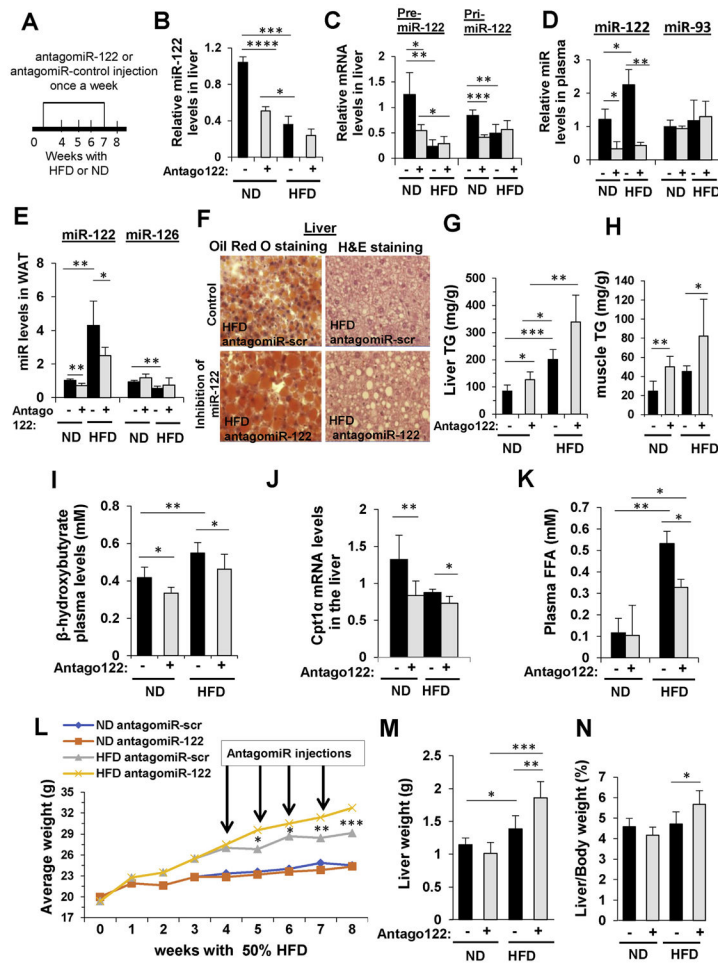


Figure 1. Inhibition of MIR122 increases steatosis in HFD-fed mice. (A) Experimental design: C57BL/6 mice were fed for 4 weeks with chow diet (ND) or 50% HFD and administered 5 μ g antagoMIR122 (Antago +) or antagomiR-scr (Antago -) once a week for 4 weeks. (B–E) qRT-PCR analysis of MIR122: (B) mature hepatic MIR122 levels, (C) hepatic pre- and pri-MIR122, and mature MIR122 levels in (D) plasma and in (E) WAT. miR-93 and miR-126 served as negative controls. (F) Oil Red O and H&E staining of liver sections. Scale bars represent 20 μ m. (G, H) Colorimetric quantification of TG levels (G) in the liver and (H) in the muscle. (I) Plasma β -hydroxybutyrate. (J) qRT-PCR analysis of hepatic Cpt1 α mRNA levels. (K) Colorimetric quantification of FFAs plasma levels. (L) Mice body weight during the treatments; arrows indicate time of antagomiR injections. (M) Liver weight. (N) Liver/body ratio measured when mice were killed. mRNA levels were normalized to hypoxanthine-guanine phosphoribosyltransferase (HPRT). Plasma microRNA levels were normalized to spiked *C elegans* miR-39; microRNA levels in the tissues were normalized to RNU6. Data are represented as mean \pm SD. n = 6. * P < .05, ** P < .01, *** P < .001, **** P < .0001. M, mol/L.

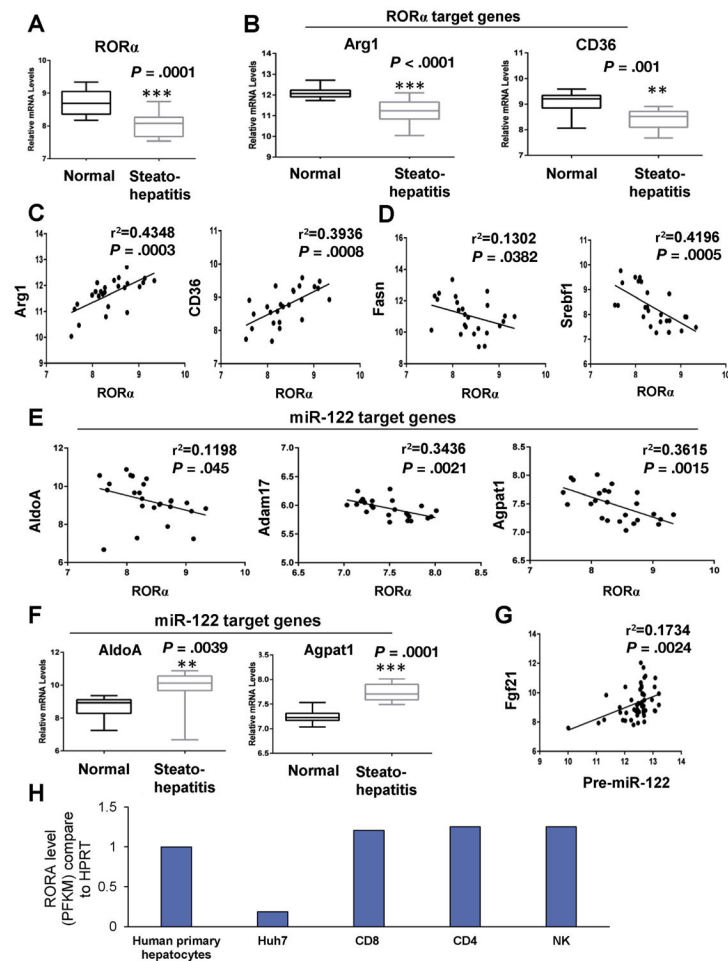


Figure 2.

Expression levels of RORA and of RORA and MIR122 target genes in livers of patients with NASH. (A–G) Database-based gene expression analysis were conducted by using human public data sets obtained from the NCBI GEO database (<http://www.ncbi.nlm.nih.gov/geo/>), processed as median-normalized signal intensity values measuring liver mRNA levels in healthy individuals and patients with steatohepatitis. (A, B) mRNA levels of RORA (*RORα*): RORA target genes (A) arginase 1 (*Arg1*) and (B) CD36. (C) Positive correlations between RORA and its target genes *Arg1* and CD36. (D) Negative correlations between RORA and genes involved in lipid metabolism: fatty acid synthase (*Fasn*) and sterol regulatory element binding transcription factor 1 (*Srebf1*). (E) Negative correlations between RORA and MIR122 target genes *AldoA*, *Adam17*, and *Agpat1*. (F) mRNA levels of MIR122 target genes in healthy individuals and patients with steatohepatitis. Correlation coefficient (r^2) were calculated by Pearson correlation test. The data represent mean \pm SD. * $P < .05$, ** $P < .01$, and *** $P < .001$ vs normal. $n = 13$ (normal) and $n = 12$ (steatohepatitis) for GEO accession number GSE33814. (G) Positive correlation between pre-MIR122 and RORA target gene (*Fgf21*) expression levels in the livers of patients with NASH. The positive correlation coefficient (r^2) was calculated by Pearson correlation test. $n = 25$ (normal) and $n = 14$ (NASH) for GEO accession number GSE89632. (H) Determination of RORA levels in hepatocytes was achieved by investigating the GSE112866 database. To

assess RORA levels in HuH7 cells, we retrieved the GSE101934 database. RORA levels in immune cells, including CD4, CD8, and NK cells, were determined by retrieving information from the GSE124731 database. RORA levels were normalized to HPRT1. As shown, RORA levels are comparable between primary human hepatocytes and immune cells. However, in Huh7 cells, the levels of RORA were approximately 20% that of hepatocytes and immune cells. FPKM, Fragments per kilobase of exon per million fragments mapped; NCBI GEO, National Center for Biotechnology Information Gene Expression Omnibus.

Author Manuscript

Author Manuscript

Author Manuscript

Author Manuscript

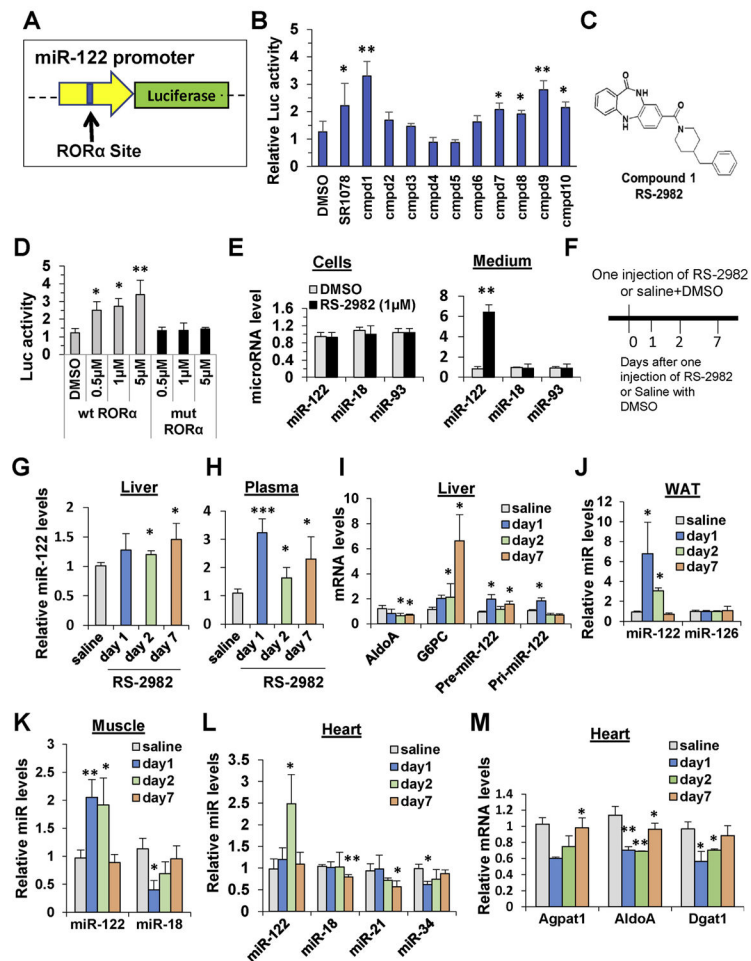


Figure 3.

A newly identified RORA agonist RS-2982 affects liver and systemic MIR122 levels in mice. (A) Schematic presentation of MIR122 promoter reporter plasmid (pMIR122 luciferase) containing the RORA binding site. (B) Huh7 cells were transfected with the pMIR122, and 1 day later, cells were treated with 1 μ mol/L of 1 of 10 different compounds. The compound solvent, 0.2% DMSO, was used as control, and 10 mol/L SR1078, a commercial RORA agonist, was used as a positive control. Luciferase activity was measured 48 hours after transfection. (C) The chemical structure of compound 1: RS-2982. (D) Huh7 cells were transfected with pMIR122 carrying a wild-type or mutated RORA binding site. One day later, cells were treated with different RS-2982 concentrations. The RS-2982 solvent, 0.2% DMSO, was used as control. Luciferase activity was measured 48 hours after transfection. Luciferase was normalized to *Renilla* luciferase activity expressed from a cotransfected pRL plasmid. (E) qRT-PCR analysis of microRNAs extracted from Huh7 cells or cell media after treatment with 1 μ mol/L RS-2982 for 24 hours. miR-18 and miR-93 served as negative controls. (F–M) The RORA agonist RS-2982 affects MIR122 expression and secretion in mice. (F) C57BL/6 mice (n = 6) were administered 7.5 mg/kg RS-2982 or saline + 5% DMSO intraperitoneally, and 1, 2, and 7 days later, mice were killed, and RNA was extracted from various tissues for qRT-PCR analysis. MicroRNA levels were measured by qRT-PCR in (G) the liver and (H) the plasma. (I) qRT-PCR analysis of pri- and pre-

MIR122, the MIR122 target gene AldoA, and the RORA target gene G6PC in the liver. (*J-L*) qRT-PCR analysis of microRNAs (*J*) in WAT, (*K*) in muscle, and (*L*) heart tissues. miR-126, miR-21, miR-34, and miR-18 levels were not increased after RS-2982 treatment. (*M*) qRT-PCR of MIR122 target genes in heart tissues. Plasma microRNA levels were normalized to spiked *C elegans* miR-39; microRNA levels in tissues were normalized to RNU6. mRNA levels were normalized to HPRT. Data are represented as mean \pm SD. * $P < .05$, ** $P < .01$. *** $P < .001$. compd, compound; M, mol/L; mut, mutated; wt, wild type.

Author Manuscript

Author Manuscript

Author Manuscript

Author Manuscript

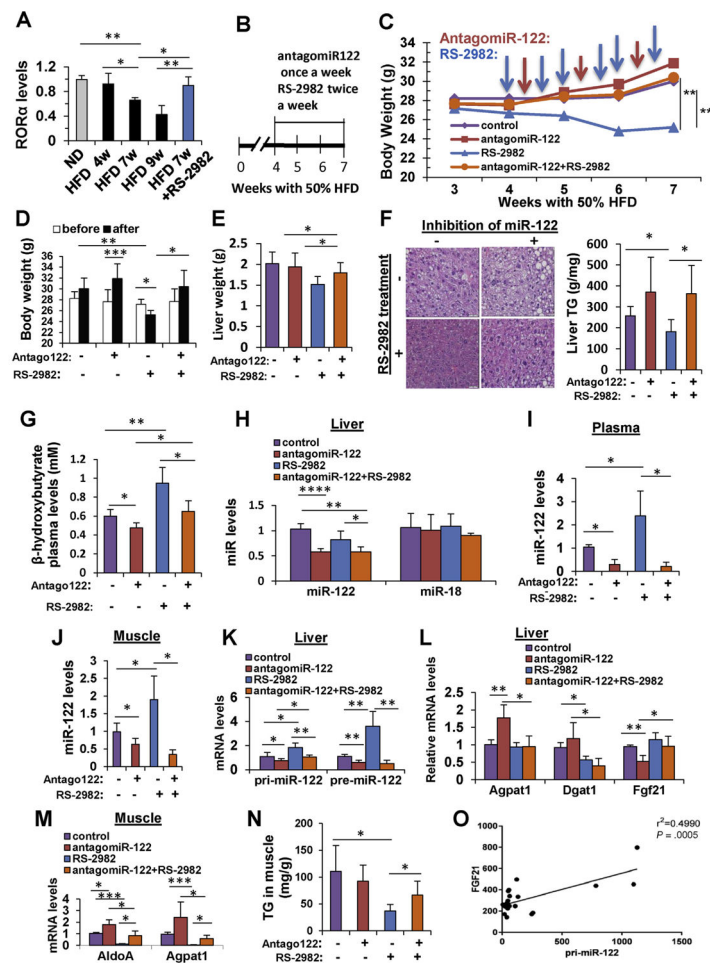


Figure 4.

The RORA agonist RS-2982 reduces steatosis via increased MIR122 expression in HFD-fed mice. (A) qRT-PCR analysis of hepatic RORα mRNA levels extracted from mice livers after 4, 7, and 9 weeks of feeding with 50% HFD. Mice that were intraperitoneally injected with 7.5 mg/kg of the RORA agonist RS-2982 after 4 weeks of HFD for 3 weeks (overall, 7 weeks under HFD feeding) show rescued RORα mRNA levels. (B) Experimental design: C57BL/6 mice were fed with HFD (to induce steatosis), and after 4 weeks, they were injected intravenously with antagomiR122 (Antago122 +) or antagomiR-control (Antago122 -) once a week, together with 7.5 mg/kg RS-2982 (or saline) intraperitoneally twice a week, for 3 weeks. (C) Mice body weight during the experiment. Blue arrows indicate the time of intraperitoneal injections of RS-2982 (or saline), and orange arrows represent the time of intravenous antagomiR (122 or control) injections. (D) Body weight before injections and after the last injection. (E) Liver weight determined at the end of the experiment. (F) H&E staining of treated mice livers (scale bars represent 20 μm); colorimetric quantification of liver TG levels. (G) Colorimetric quantification of plasma β-hydroxybutyrate. (H–J) qRT-PCR analysis of mature MIR122 (H) in the liver (control miR-18 levels were not affected after RS-2982 treatment), (I) plasma MIR122 levels, and (J) muscle. (K) pri-MIR122 and pre-MIR122 in the liver. (L) MIR122 (Agpat1 and Dgat1) and RORA (Fgf21) target genes in the liver. (M) MIR122 target genes (Aldoa and Agpat1) in

the muscle. (*N*) Muscle TG content in the described treatments. Supplementary Table 6 shows that pri-MIR122 is not expressed in muscle tissue. (*O*) RNA-sequencing analysis of RNA extracted from liver tissues showing a positive correlation between pri-MIR122 and Fgf21 (RORA target gene) mRNA expression. Plasma microRNA levels were normalized to spiked *C elegans* miR-39; microRNA levels in the tissues were normalized to RNU6. mRNA levels were normalized to HPRT. Data are represented as mean \pm SD. n = 6. * $P < .05$, ** $P < .01$ *** $P < .001$, **** $P < .0001$.

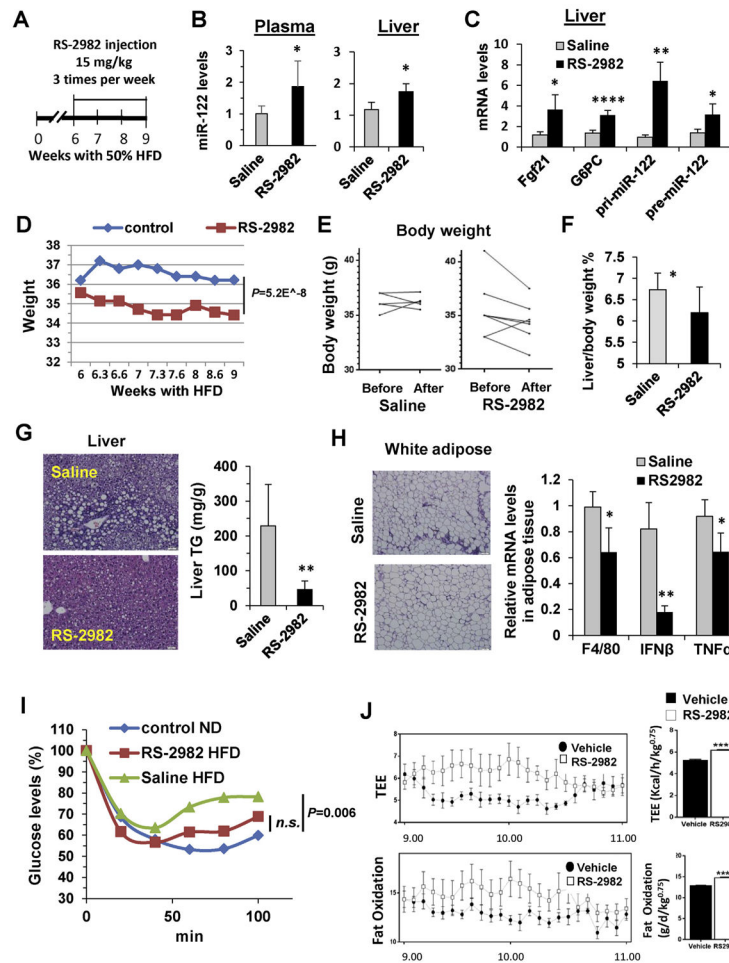


Figure 5.

The RORA agonist RS-2982 reverses NAFLD in mice. (A) Experimental design: C57BL/6 mice were fed with 50% HFD, and after 6 weeks, they were injected with 15 mg/kg RS-2982 (or saline + DMSO) 3 times a week for an additional 3 weeks (n = 5 for saline and n = 7 for RS-2982). (B) qRT-PCR analysis of MIR122 extracted from plasma and from liver. (C) qRT-PCR analysis of RORA target genes and pri- and pre-MIR122 mRNA extracted from mice livers. (D) Body weight measured during the experiment. (E) Body weight per mouse before and after treatment. (F) Liver/body weight ratio (%) measured at the end of the experiment. (G) Liver H&E staining and colorimetric quantification of liver TG levels. Scale bars represent 10 μ m. (H) H&E staining of adipose tissue and qRT-PCR analysis of mRNA of inflammation-related genes extracted from adipose tissue. (I) Whole-blood glucose levels during an insulin tolerance test in HFD-fed RS-2982–treated mice vs HFD-fed saline-treated mice and ND fed mice (control ND); minutes indicate the time after insulin injection. (J) Metabolic cages: after 2 weeks of RS-2982 or saline + DMSO (vehicle) treatment, mice were monitored by the Promethion High-Definition Behavioral Phenotyping System (Sable Instruments) over a 24-hour period. Note an increased total energy expenditure and fat oxidation in the RS-2982–treated mice compared with saline + DMSO (vehicle)–treated animals at a specific time zone. Effective mass was calculated by a power of 0.75. Data are

mean \pm standard error of the mean from 8 mice per group. IFN, interferon; n.s., not significant; TEE, total energy expenditure; TNF, tumor necrosis factor;

Author Manuscript

Author Manuscript

Author Manuscript

Author Manuscript

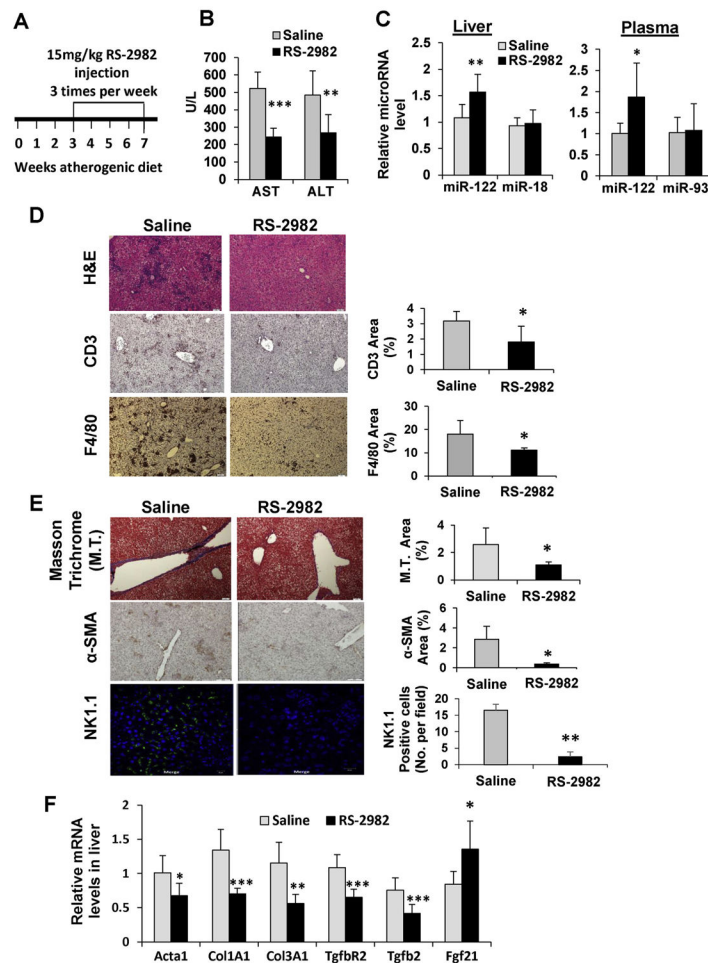


Figure 6.

The anti-inflammatory and anti-fibrogenic effects of RS-2982. (A) Experimental design: C57BL/6 mice were fed with atherogenic diet (to induce fibrosis), and after 3 weeks they were injected with 15 mg/kg RS-2982 (or saline + DMSO) 3 times a week for additional 3.5 weeks ($n = 8$). (B) Plasma levels of ALT and AST liver enzymes measured at the end of the experiment. (C) qRT-PCR analysis of microRNAs extracted from liver and plasma. miR-18 and miR-93 served as negative controls. (D, E) Representative microphotographs of stained livers taken from saline or RS-2982-treated mice. (D) Staining for H&E, CD3, and F4/80; (E) Masson trichrome, α -SMA, and anti-NK1.1 (green) stained livers. Merged fluorescence images with DAPI (blue). Scale bars represent 10 μ m. The graphs on the right of the microphotographs show quantification of positively stained areas using ImageJ (National Institutes of Health, Bethesda, MD). (F) qRT-PCR analysis of mRNA of genes involved in fibrosis and the RORA target gene (Fgf21) extracted from mice livers. Plasma microRNA levels were normalized to spiked *C elegans* miR-39; microRNA levels in the tissues were normalized to RNU6. mRNA levels were normalized to HPRT. Data are represented as mean \pm SD. * $P < .05$, ** $P < .01$, *** $P < .001$. ALT, alanine aminotransferase; AST, aspartate aminotransferase; DAPI, 4',6-diamidino-2-phenylindole; M.T., Masson trichrome; SMA, smooth muscle actin.

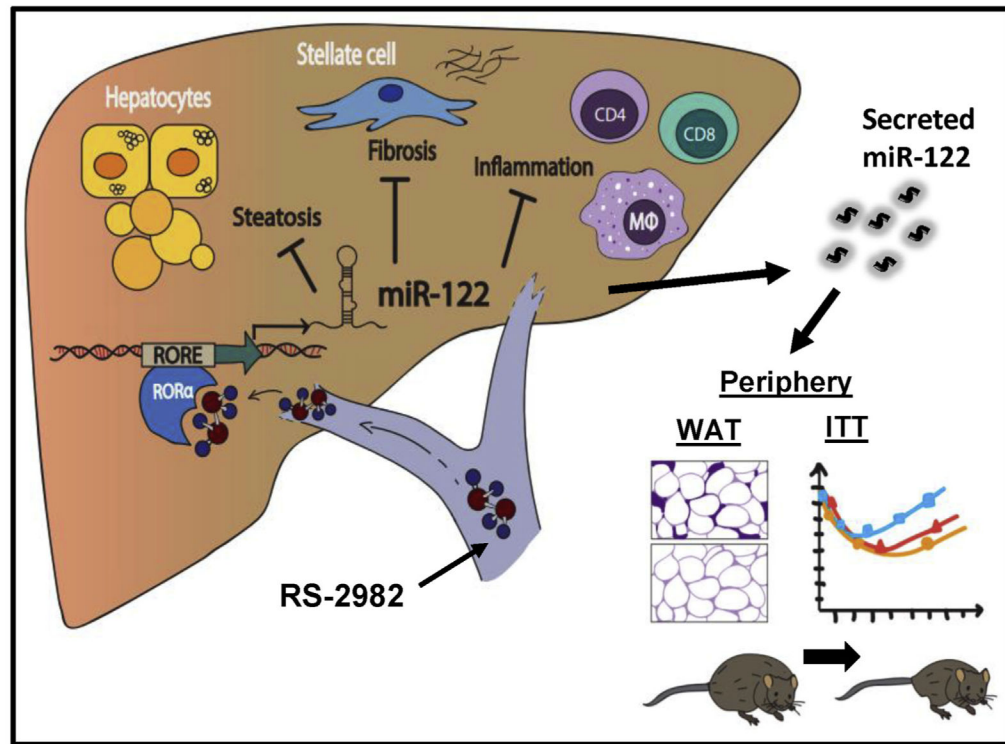


Figure 7.

Our suggested model for reversal of NAFLD by activation of MIR122. Administration of RS-2982, which binds and activates the RORA transcription factor in the liver, leads to increased MIR122 levels in the liver and blood. This, in turn, reduces TG levels in the liver and muscle tissues, decreases inflammation and fibrosis in the liver, culminating in increased wholebody energy expenditure, increased fat-oxidation and insulin sensitivity, and reduced weight and inflammation in adipose tissue.